Lyapunov exponents of systems with elastic hard collisions

Ch. Dellago* and H. A. Posch†
Institut für Experimentalphysik, Universität Wien, Strudlhofgasse 4, A-1090 Wien, Austria
(Received 7 March 1995)

Benettin's classical method for the calculation of the Lyapunov exponent spectra of smooth flows is applied to the case of systems with elastic hard collisions. As illustrative examples the maximum Lyapunov exponent is calculated for the two-dimensional periodic Lorentz gas over a wide density range, and for the Sinai stadium billiard.

PACS number(s): 05.45.+b, 02.70.−c, 05.20.−y

I. INTRODUCTION

A useful way to characterize and quantify chaotic phenomena arising in dynamical systems is by means of the so-called Lyapunov exponents, which describe the temporal evolution of small perturbations of the initial conditions. For the calculation of complete Lyapunov-exponent spectra of autonomous systems of ordinary differential equations the algorithm of Benettin *et al.* has become a well established method [1,2]. Our goal in this paper is to develop a scheme for the application of this method to systems with elastic hard collisions, like billiards, hard sphere fluids, or the Lorentz gas. In order to define the concepts and terms we are going to use in the following paragraphs, we give a brief overview of the classical algorithm mentioned above.

Let us consider a dynamical system given by N coupled first-order differential equations:

$$\dot{\mathbf{\Gamma}}(t) = \mathbf{F}(\mathbf{\Gamma}(t)). \tag{1}$$

Since we are interested in the time evolution of a small perturbation $\boldsymbol{\delta}(t)$ of a trajectory $\mathbf{\Gamma}(t)$, we linearize the equations of motion obtaining

$$\dot{\boldsymbol{\delta}}(t) = \left.\frac{\partial \mathbf{F}}{\partial \mathbf{\Gamma}}\right|_{\mathbf{\Gamma}=\mathbf{\Gamma}(t)} \cdot \boldsymbol{\delta}(t) \tag{2}$$

for the temporal evolution of the vectors $\boldsymbol{\delta}(t)$ in the tangent bundle of the system. $\boldsymbol{\delta}(t)$ will be referred to as an *offset vector*, $\mathbf{\Gamma}(t)$ is the trajectory in phase space, and $\mathbf{D} = \partial\mathbf{F}/\partial\mathbf{\Gamma}$ is the $N \times N$ Jacobi matrix of the system. Obviously, the matrix $\mathbf{D}$ depends on the instantaneous phase $\mathbf{\Gamma}(t)$.

Formally the solution of the system (2) can be written as

$$\boldsymbol{\delta}(t) = \mathbf{L}(t;0)\boldsymbol{\delta}(0), \tag{3}$$

where $\mathbf{L}(t;0)$ is the propagator for the offset vector $\boldsymbol{\delta}(t)$ and is given by the time-ordered exponential

$$\mathbf{L}(t;0) = \exp_+\left\{\int_0^t \mathbf{D}(\mathbf{\Gamma}(t'))dt'\right\}. \tag{4}$$

For ergodic systems obeying very general assumptions Oseledec [3] has shown that for almost every initial condition of the trajectory there exists a set of offset vectors $\boldsymbol{\delta}_i(t)$, $i = 1, \ldots, N$, such that the numbers

$$\lambda_i = \lim_{T\to\infty} \frac{1}{T} \ln \frac{|\mathbf{L}(T;0)\boldsymbol{\delta}_i(0)|}{|\boldsymbol{\delta}_i(0)|} \tag{5}$$

exist and are independent of the initial conditions. These numbers give the logarithmic contraction or expansion rates in different directions of phase space, and are independent of the coordinate system and the metric. Their whole set is called the Lyapunov spectrum of the system. An initial perturbation of a trajectory in a direction corresponding to a positive Lyapunov exponent tends to grow exponentially, which means that the offset vector $\boldsymbol{\delta}(t)$ for a neighboring trajectory, differentially separated from the reference trajectory $\mathbf{\Gamma}(t)$, diverges exponentially with $t \to \infty$. Conversely, trajectories separated by an infinitesimally small vector in a direction with negative Lyapunov exponent converge exponentially. A dynamical system with at least one positive Lyapunov exponent is called chaotic. As usual we order the Lyapunov spectrum such that $\lambda_1 \geq \lambda_2 \geq \cdots \geq \lambda_N$.

For the calculation of the Lyapunov spectrum according to the above mentioned method it is necessary to integrate simultaneously the equations of motion (1) for the reference trajectory $\mathbf{\Gamma}(t)$ and for N complete equation systems (2) for the offset vectors $\boldsymbol{\delta}_i(t)$, $i = 1, \ldots, N$. If the vector function $\mathbf{F}(\mathbf{\Gamma}(t))$ and the matrix $\mathbf{D}(\mathbf{\Gamma}(t))$ are smooth functions of their argument, this task may be accomplished by any standard integrator [4]. Since the offset vectors grow with exponential rates and, moreover, tend to align in the direction of the eigenvector of $\mathbf{L}(t;0)$ associated with the largest eigenvalue, they must be periodically reorthonormalized [1,2]. The Lyapunov exponents can then be obtained from the time average of the logarithm of the respective renormalization factors.

This method has been applied to a great number of different dynamical systems with phase space dimension N ranging from $N = 3$ to $N = 400$ for the evaluation of the full spectrum [5], and to $N = 129600$ for the maximum

*Electronic address: dellago@ls.exp.univie.ac.at
†Electronic address: posch@ls.exp.univie.ac.at

exponent [6]. But all these systems have in common that their temporal evolution is governed by an equation like (1) with a differentiable function $\mathbf{F}(\mathbf{\Gamma})$. If this smoothness condition is not fulfilled due to the occurrence of a hard-wall potential, a straightforward application of the method is not possible. In order to overcome this problem we propose a new scheme, which allows the calculation of Lyapunov exponents in systems with hard-core interactions as well as in hybrid systems with a mixture of smooth and hard-core interactions. After the description of this method in Sec. II we apply it in Sec. III to the two-dimensional periodic Lorentz gas with scatterers on a triangular lattice, and to the famous Sinai stadium billiard.

II. METHOD

For the sake of simplicity and without loss of generality, we consider a point particle in two dimensions whose motion is described almost always by an equation of type (1). At discrete times the particle collides with a hard, generally curved obstacle, which causes both the trajectory and the offset vectors to change in a noncontinuous way. In the following we assume the border of the obstacle to be at least piecewise smooth. Figure 1 shows the geometry of such a collision, where $\mathbf{p}$ is the momentum of the particle immediately before the collision, and $\mathbf{p}'$ immediately after the collsion. The vectors $\mathbf{t}$ and $\mathbf{t}'$ are unit vectors, which are normal to $\mathbf{p}$ and $\mathbf{p}'$, respectively, and which can be generated from the momentum vectors through a $\pi/2$-anticlockwise rotation $D^{\pi/2}$:

$$\mathbf{t} = \frac{1}{|\mathbf{p}|} D^{\pi/2}\mathbf{p} \qquad \mathbf{t}' = \frac{1}{|\mathbf{p}'|} D^{\pi/2}\mathbf{p}'. \tag{6}$$

The obstacle is given by a curve $\mathbf{k}(s)$, which is parametrized with the arclength s. The vector $\mathbf{u} = \dot{\mathbf{k}}(s)$ is tangent to the obstacle in the collision point, and is also a unit vector. In the following the curvature of the obstacle is of crucial importance in our considerations. It is defined as the rate of change of the tangent-vector orientation with growing arclength, and is denoted by κ. For a curve parametrized with the arclength κ is equal to the magnitude of the second derivative of $\mathbf{k}(s)$ with respect to s:

$$\kappa = \left|\ddot{\mathbf{k}}(s)\right|. \tag{7}$$

By normalizing the curvature vector $\ddot{\mathbf{k}}(s)$ one obtains the principal normal vector $\mathbf{h}(s) = \ddot{\mathbf{k}}(s)/\kappa$. With these definitions we can write down the effect of a hard elastic collision on the offset vectors $\boldsymbol{\delta} \equiv \{\delta\mathbf{q}, \delta\mathbf{p}\}$. First we note that the reference trajectory undergoes the following noncontinuous change:

$$\begin{aligned} \mathbf{q} &\rightarrow \mathbf{q}, \\ \mathbf{p} &\rightarrow \mathbf{p}'. \end{aligned} \tag{8}$$

Here, and in the following expressions the specular reflection of a vector on the tangent in the collision point is denoted by a prime. Obviously the position of the particle is the same immediately before and after the collision, whereas the momentum of the particle is simply reflected on the obstacle. Next we consider the position components $\delta\mathbf{q} \equiv \{\delta x, \delta y\}$ of the offset vector $\boldsymbol{\delta}$. Neglecting quantities of second order and noting that the vector $\delta\mathbf{q}''$ vanishes at the collision, one infers from Fig. 2 that

$$\delta\mathbf{q} \rightarrow \delta\mathbf{q}', \tag{9}$$

which corresponds to a simple reflection at the collision point. In calculating the effect of the collision on the momentum components $\delta\mathbf{p} \equiv \{\delta p_x, \delta p_y\}$ of the offset vector it is necessary to account for the fact that a displacement $\delta\mathbf{q}$ in the configuration space leads to a collision point, which is displaced by the arclength δs from the collision point of the reference trajectory. This causes a change in the direction of the outgoing momentum and generates an additional term $\delta\mathbf{p}''$ (see Fig. 2) in the expression for the vector $\delta\mathbf{p}$ after the collision. It follows from the definition of the curvature, that the orientation of the

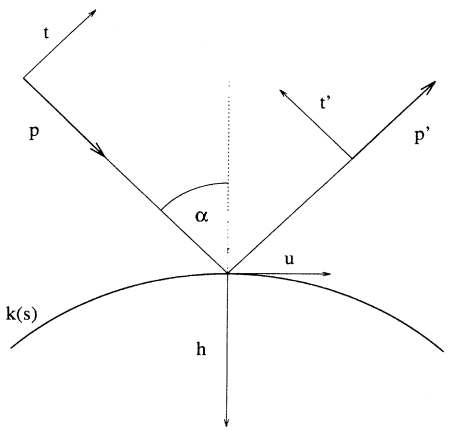

FIG. 1. The collision geometry.

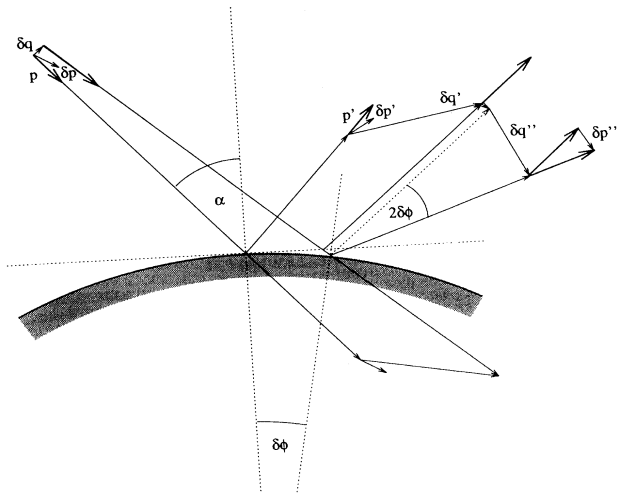

FIG. 2. The effect of a collision on the offset vector $\boldsymbol{\delta}$.

tangent and therefore also of the principal normal vector changes by the (inifinitesimal) angle $\delta\phi$:

$$\delta\phi = \kappa\delta s. \tag{10}$$

Since both the angle of incidence and angle of reflection are altered by $\delta\phi$, we obtain

$$\delta\mathbf{p} \to \delta\mathbf{p}' - 2\delta\phi\,|\mathbf{p}|\,\mathbf{t}'. \tag{11}$$

The first term on the right hand side corresponds to a simple specular reflection on the tangent and is independent of the curvature and the spatial component $\delta\mathbf{q}$ of the offset vector. The second term is a consequence of the rotation of the outgoing momentum of the displaced trajectory with respect to the outgoing momentum of the reference trajectory. Taking into account that the displacement δs along the obstacle is given by

$$\delta s = \frac{\delta\mathbf{q}\cdot\mathbf{t}}{\cos\alpha} = \frac{\delta\mathbf{q}\cdot\mathbf{t}}{\mathbf{p}\cdot\mathbf{h}}\,|\mathbf{p}| \tag{12}$$

the momentum components are changed by the hard collision according to

$$\delta\mathbf{p} \to \delta\mathbf{p}' - 2\kappa\frac{\delta\mathbf{q}\cdot\mathbf{t}}{\mathbf{p}\cdot\mathbf{h}}\,|\mathbf{p}|^2\,\mathbf{t}'. \tag{13}$$

Equations (1) and (2) give us the temporal evolution of the system between hard collisions, and the relations (8), (9), and (13) tell us how the configuration-space components $\delta\mathbf{q}$ and the momentum-space components $\delta\mathbf{p}$ of the offset vector $\boldsymbol{\delta}$ change during an instantaneous hard elastic collision with a curved surface. The results (9) and (13) are accurate to first order as required for the evaluation of Lyapunov exponents and can be easily incorporated in the standard algorithm described in the Introduction. It should be clear that our method is the exact limiting case of the algorithm working with finite distances between neighboring trajectories in phase space and that the dynamics specified by (8), (9), and (13) occurs in tangent space.

III. APPLICATIONS

A. The periodic Lorentz gas

We consider a point particle of mass $m = 1$, the so-called wanderer, moving in a plane between hard disks with radius $R = 1$, their centers being fixed on the sites of a regular triangular lattice (see Fig. 3). Between the hard collisions, which are assumed to be elastic, the wanderer moves freely and with constant velocity. Since the Lyapunov exponent of such a system is obviously proportional to the velocity of the wanderer, it is sufficient to consider one single velocity, and we take $v = 1$. For $R = 1$ the geometry of the system is completely defined by the density $\rho = 1/A$, where A is the area of the hexagonal unit cell of the triangular lattice (to avoid confusion we note that in Ref. [7] the density is defined as precisely twice our value). In what follows we allow the hard scatterers to intersect each other. This can be justified by the

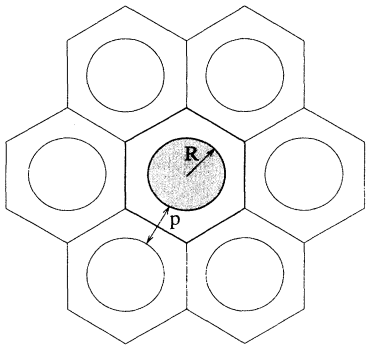

FIG. 3. The geometry of the periodical 2D Lorentz gas. R is the radius of the scatterer and p denotes the unstable periodic orbit discussed in the text. In all simulations reduced units are used for which the scatterer radius R, the wanderer velocity v, and the wanderer mass m are unity.

observation that the system described above is equivalent to a system, in which all scatterers as well as the wanderer are replaced by hard disks with radius $R' = R/2$. For such high densities the free volume accessible to the wanderer is obviously separated into disjoint cells.

In the time between the collisions the wanderer moves according to the free-particle Hamiltonian $H = (p_x^2 + p_y^2)/2m$:

$$\begin{aligned} \mathbf{q} &= \mathbf{q}_0 + \mathbf{p}_0 t, \\ \mathbf{p} &= \mathbf{p}_0, \end{aligned} \tag{14}$$

where $\mathbf{q}_0$ and $\mathbf{p}_0$ are the respective position and momentum of the wanderer immediately after the last collision, and t is the time passed since then. The offset vectors evolve according to

$$\boldsymbol{\delta} = \begin{cases} \delta\mathbf{q} &= \delta\mathbf{q}_0 + \delta\mathbf{p}_0\, t, \\ \delta\mathbf{p} &= \delta\mathbf{p}_0, \end{cases} \tag{15}$$

where $\delta\mathbf{q}_0$ and $\delta\mathbf{p}_0$ are the respective position and momentum components of $\boldsymbol{\delta}(t)$ immediately after the last collision. The effect of the hard collision on the trajectory of the wanderer is given by Eq. (8), which correponds simply to a specular reflection. In order to apply Eqs. (9) and (13) we observe that the curvature of the circular scatterers $\kappa = 1/R$, and we obtain

$$\delta\mathbf{p} \to \delta\mathbf{p}' - \frac{2}{R}\frac{\delta\mathbf{q}\cdot\mathbf{t}}{\cos\alpha}\,|\mathbf{p}|\,\mathbf{t}'. \tag{16}$$

Here, α is the angle of incidence of the wanderer. With these expressions we are now able to calculate the spectrum of Lyapunov exponents with Benettin's classical algorithm. The phase space is four dimensional, but two of the Lyapunov exponents vanish due to the energy conservation and the fact that a perturbation in the direction of the phase flow does not exhibit exponential growth or decay. Due to the symplectic nature of our system the two remaining exponents are of equal size and opposite sign and form a *Smale pair* [8]. The sum of all Lyapunov exponents vanishes as required by Liouville's theorem. Thus, it suffices to evaluate the maximum ex-

ponent. Nevertheless the fulfillment of these symmetry conditions for the complete spectra may be regarded as a useful numerical test for the algorithm. In all our simulations these properties of the Lyapunov spectrum have been checked and verified.

Figure 4 shows the maximum Lyapunov exponent λ_1 of the periodic Lorentz gas as a function of density. The numerical convergence of the algorithm is rather good: after about 10^5 collisions the relative error in the Lyapunov exponent is less then 0.25%. In Fig. 4 the number of collisions per run varied from 10^5 at low densities to 10^7 at high densities. Three special densities are marked by vertical broken lines. Systems with a density below $\rho_0 = \sqrt{3}/8 \simeq 0.2165$ have an infinite horizon, whereas the horizon is finite for densities greater than ρ_0. If the density exceeds $\rho_1 = \sqrt{3}/6 \simeq 0.2887$, the wanderer is confined to a single cage formed by the scatterer and the diffusion constant vanishes. ρ_1 is referred to as the close packed density of the scatterers. We observe a slight change in the functional form of $\lambda_1(\rho)$ as ρ passes through ρ_1. Finally, the density $\rho_2 = 2\sqrt{3}/9 \simeq 0.3849$ corresponds to the density, for which the free volume accessible to the wanderer vanishes. If the density approaches this limiting value, the collision rate and therefore also the Lyapunov exponent diverge.

In a recent paper van Beijeren and Dorfman [9], using a Lorentz-Boltzmann equation, presented a calculation of the Lyapunov exponent of the Lorentz gas with random scatterers for the limiting case of low densities. They obtain

$$\lambda = 2\rho R v[1 - \ln 2 - C - \ln(\rho R^2)] \quad \text{for } \rho \ll 1, \qquad (17)$$

where v is the velocity of the wanderer and $C \simeq 0.577216$ is Euler's constant. A comparison of this expression (full line) with our results (diamonds) for low densities is shown in Fig. 5. The agreement of the results is satisfactory even if the analytical estimate (17) assumes a random distribution of scatterers, whereas our results correspond to a regular lattice of scatterers. The relative difference between the results approaches zero in the limit $\rho \to 0$. We calculated also the maximum Lyapunov exponent for a system of 10000 randomly distributed scatterers with periodical boundary conditions. As in Ref. [9] the scatterers are not allowed to overlap and the Lyapunov exponents are obtained by averaging over different random configurations of scatterers. The results of this calculation are shown in Fig. 5 and are marked by filled squares. For small densities the results agree perfectly with the Lorentz-Boltzmann-equation approach of van Beijeren and Dorfman [9]. It is interesting to note that the Lyapunov exponents for different random scatterer configurations differ by about 0.1%.

Stoddard and Ford [10] derived an approximate expression for λ_1 for a system of hard particles. It is surprising that their rough estimate leads to exponents in rather close agreement with our model for densities $\rho < 0.005$. For larger densities their numbers deviate significantly to more negative values.

Another check of our algorithm is possible by evaluating the Lyapunov exponents of unstable periodic orbits described in [11]. In this paper the authors consider the simple periodic orbit of the wanderer bouncing between two scatterers, which is denoted with p in Fig. 3. They obtain

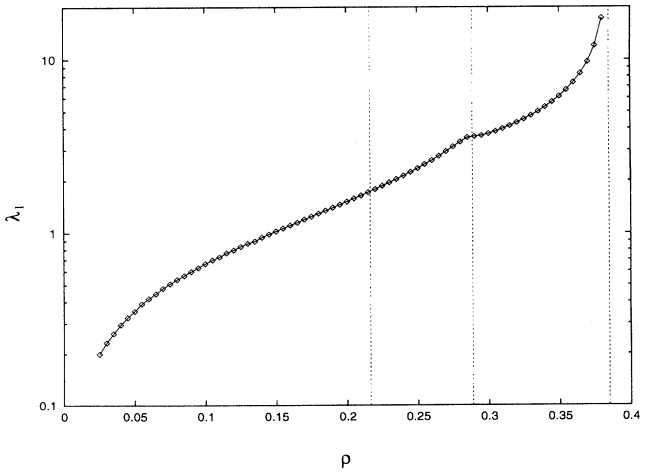

FIG. 4. Maximum Lyapunov exponent λ_1 vs density ρ in the periodical 2D Lorentz gas. The three vertical broken lines mark the densities ρ_0 (transition from infinite to finite horizon), ρ_1 (wanderer confined to the cage), and ρ_2 (zero free volume for the wanderer), respectively, as discussed in the text. Reduced units are used for which the scatterer radius R, the wanderer velocity v, and the wanderer mass m are unity.

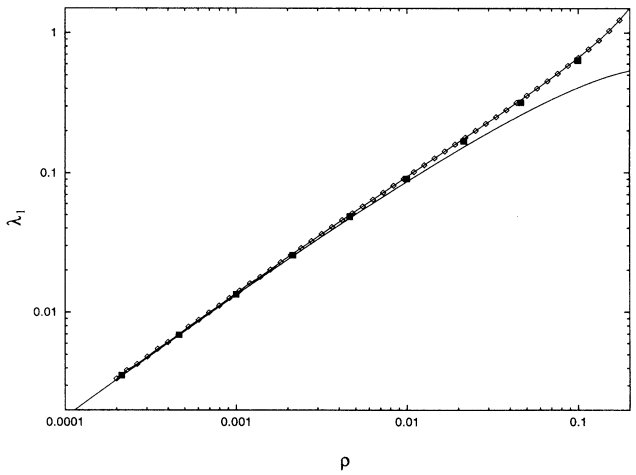

FIG. 5. Lyapunov exponent λ_1 at low densities ρ in the periodical 2D Lorentz gas. The full line is the approximation of van Beijeren and Dorfman [9] for a system of randomly distributed scatterers, the diamonds are our numerical results for a periodic arrangement of scatterers (see text). The filled squares are the results for a numerical simulation with randomly distributed scatterers and periodical boundary conditions. In this simulation the maximum Lyapunov exponent λ_1 has been calculated as an average over 10 different random configurations of 10000 scatterers, which where not allowed to overlap. Reduced units are used for which the scatterer radius R, the wanderer velocity v, and the wanderer mass m are unity.

$$\lambda = \frac{v}{a-2R} \ln \frac{a-R+\left(a^2-2Ra\right)^{1/2}}{R}, \tag{18}$$

where a is the distance between the centers of the two reflecting disks. The results of our numerical simulation are in excellent agreement with this expression.

There is also another method by Sinai [12,13] for the evaluation of maximum Lyapunov exponent of the Lorentz gas. It is based on the curvature of a "wave front" expanding in the system of scatterers. Other attempts are based on an expansion of the dynamics in terms of unstable periodic orbits both in equilibrium [14,7] and in nonequilibrium steady states [15,16]. Our method is more versatile and exact. It may be used for the calculation of the full spectrum of exponents and may easily be generalized to higher dimensions.

B. The stadium billiard

As a second illustrative example we apply our recipe to the so-called Sinai stadium billiard [12,17–19]. This simple model is a special case of a *billiard system*, which generally consists of a point particle moving inside a two-dimensional domain Q with closed boundary ∂Q. Inside Q the particle moves freely with constant velocity $v = 1$. At collisions with the boundary ∂Q the particle is reflected elastically. The border of the stadium billiard consists of two arcs of radius R connected by two parallel segments with length $2a$ and is schematically depicted in Fig. 6. The circular components have a *focusing* effect on a set of neighbouring trajectories, whereas the linear parts are *neutral* in this context. In the case of $a > 0$ the initially focused trajectories are dispersed after reaching the so-called *conjugate point* leading to a net dispersing effect and therefore to chaotic motion. It can be proved that for $a = 0$ the system is completely integrable. For $a > 0$ it is a K system and has a positive Lyapunov exponent [20].

As in the case of the Lorentz gas the trajectory and the offset vectors evolve according to Eqs. (14) and (15) in the time between successive collisions with the border. At the collision with the border the particle is reflected elastically and the effect of the collision on the offset vetors is again described by Eqs. (9) and (13). Since the collision takes place on the inner side of the border, we obtain the following expression for the position and momentum components of the offset vector:

$$\begin{aligned} \delta\mathbf{q} &\rightarrow \delta\mathbf{q}', \\ \delta\mathbf{p} &\rightarrow \delta\mathbf{p}' + 2\kappa \tfrac{\delta\mathbf{q}\cdot\mathbf{t}}{\cos\alpha} |\mathbf{p}| \mathbf{t}'. \end{aligned} \tag{19}$$

If the collision takes place in the curved part of the border, the curvature $\kappa = 1/R$. On the linear parts of the border the curvature κ vanishes.

With these expressions we calculated the maximum Lyapunov exponent for a range of the parameter $\gamma = a/R$. As before it is sufficient to consider the case $v = 1$. As can be seen by similarity considerations, the Lyapunov exponents of systems with the same ratio γ but different size are related by [17]

$$\lambda(\gamma, A') = \sqrt{A/A'}\,\lambda(\gamma, A), \tag{20}$$

where $A(a,R) = 4aR + \pi R^2$ is the area of the domain Q. In Fig. 7 we show λ_1 as a function of $\gamma = a/R$ for a constant area $A = A(1,1)$. The number of collisions with the wall is approximately 5×10^7 for each run. Our results reproduce exactly those of Benettin and Strelcyn [17], who calculated the maximum Lyapunov exponent with *finite* instead of *differential* offset vectors. Our method of differential vectors is more elegant and—in addition—offers an increase in performance since in the finite difference case the collision point must be determinded both for the reference trajectory and the trajectories displaced by a small but finite vector. Our results agree also with the results of a recent paper [21], in which the authors have calculated the maximum Lyapunov exponent by averaging over unstable periodic orbits. As one can infer from Fig. 7 the maximum Lyapunov exponent vanishes for $\gamma = 0$ and increases very rapidly for $\gamma > 0$. It reaches its maximum value in the range $\gamma = 1.2 - 1.4$. The

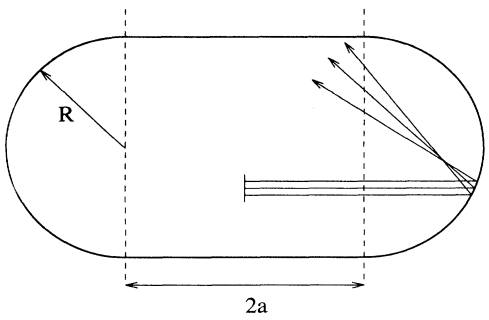

FIG. 6. Geometry of the stadium billiard.

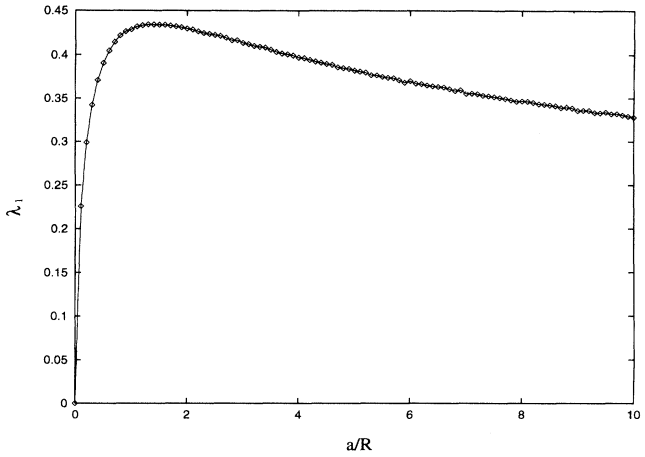

FIG. 7. Lyapunov exponent in the stadium billiard vs $\gamma = a/R$ for constant area $A = A(1,1)$ of the billiard.

limit $\gamma \to \infty$ corresponds to an integrable system, and λ_1 should vanish again.

IV. CONCLUSION

We have presented a simple method for the calculation of the full set of Lyapunov exponents in systems with elastic hard collisions. The application of our method to dissipative systems is straightforward. This means that nonequilibrium systems in stationary states, like the Lorentz gas with external field and thermostat [22,23], can be easily treated with our algorithm [24]. Finally, we want to mention that Lyapunov exponent spectra can be calculated also for hard sphere fluids in equilibrium and nonequilibrium conditions, as will be shown in future work.

ACKNOWLEDGMENTS

We gratefully acknowledge the financial support from the Fonds zur Förderung der wissenschaftlichen Forschung, Grant No. P09677, and the generous allocation of computer resources by the Computer Center of the University of Vienna. We thank J. R. Dorfman, L. Glatz, W. G. Hoover, and B. Holian for their interest in our work and for useful discussions, and G. P. Morriss for communicating Ref. [16].

[1] G. Benettin, L. Galgani, A. Giorgilli, and J.-M. Strelcyn, Meccanica **15**, 9 (1980).
[2] A. Wolf, J. B. Swift, H. L. Swinney, and J. A. Vastano, Physica D **16**, 285 (1985).
[3] V. I. Oseledec, Trans. Moscow Math. Soc. **19**, 197 (1968).
[4] F. J. Vesely, *Computational Physics, An Introduction* (Plenum, New York, 1994).
[5] W. G. Hoover and H. A. Posch, Phys. Rev. E **49**, 1913 (1994).
[6] W. G. Hoover and H. A. Posch, Phys. Rev. E **51**, 273 (1995).
[7] G. P. Morriss and L. Rondoni, J. Stat. Phys. **75**, 553 (1994).
[8] H. A. Posch and W. G. Hoover, Phys. Rev. A **38**, 473 (1988).
[9] H. van Beijeren and J. R. Dorfman, Phys. Rev. Lett. **74**, 1319 (1995).
[10] S. D. Stoddard and J. Ford, Phys. Rev. A **8**, 1504 (1973).
[11] P. Gaspard and G. Nicolis, Phys. Rev. Lett. **65**, 1693 (1990).
[12] Ya. G. Sinai, Russ. Math. Surv. **25**, 137 (1970).
[13] P. Gaspard and F. Baras, in *Microscopic Simulations of Complex Hydrodynamic Phenomena*, edited by M. Mareshal and B. Holian (Plenum, New York, 1992).
[14] P. Cvitanovic, P. Gaspard, and T. Schreiber, Chaos **2**, 85 (1992).
[15] W. N. Vance, Phys. Rev. Lett. **69**, 1356 (1992).
[16] J. Lloyd, M. Niemeyer, L. Rondoni, and G. P. Morriss, Chaos (to be published).
[17] G. Benettin and J.-M. Strelcyn, Phys. Rev. A **17**, 773 (1978).
[18] L. A. Bunimovich, Commun. Math. Phys. **65**, 295 (1979).
[19] L. A. Bunimovich, Ya. G. Sinai, and N. J. Chernov, Russ. Math. Surv. **46**, 47 (1991).
[20] L. A. Bunimovich, Funct. Anal. Appl. **8**, 254 (1974).
[21] O. Biham and M. Kvale, Phys. Rev. A **46**, 6334 (1992).
[22] W. G. Hoover, B. Moran, C. G. Hoover, and W. J. Evans, Phys. Lett. A **133**, 114 (1988).
[23] N. J. Chernov, G. L. Eyink, J. L. Lebovitz, and Ya. G. Sinai, Commun. Math. Phys. **154**, 569 (1993).
[24] Ch. Dellago, L. Glatz, and H. A. Posch, Phys. Rev. E (to be published).

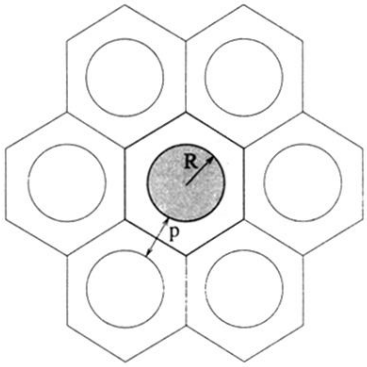

FIG. 3. The geometry of the periodical 2D Lorentz gas. R is the radius of the scatterer and p denotes the unstable periodic orbit discussed in the text. In all simulations reduced units are used for which the scatterer radius R, the wanderer velocity v, and the wanderer mass m are unity.